An Unexpected Pathway for the Catalytic Oxidation of Methylidyne on Rh{111} as a Route to Syngas

ARTICLE *in* JOURNAL OF THE AMERICAN CHEMICAL SOCIETY · MARCH 2007

Impact Factor: 12.11 · DOI: 10.1021/ja067722w · Source: PubMed

3 AUTHORS, INCLUDING:

Oliver R Inderwildi
University of Oxford
48 PUBLICATIONS **1,067** CITATIONS
SEE PROFILE

Stephen John Jenkins
University of Cambridge
151 PUBLICATIONS **2,852** CITATIONS
SEE PROFILE

J|A|C|S
ARTICLES
Published on Web 01/23/2007

An Unexpected Pathway for the Catalytic Oxidation of Methylidyne on Rh{111} as a Route to Syngas

Oliver R. Inderwildi,* Stephen J. Jenkins, and David A. King

Contribution from the University of Cambridge, Department of Chemistry, Lensfield Road, Cambridge CB2 1EW, United Kingdom

Received November 3, 2006; E-mail: ori20@cam.ac.uk

Abstract: This study investigates the adsorption properties of methylidyne (CH) on Rh{111}, its partial and full oxidation as well as its surface mobility, by means of plane-wave density functional theory (DFT) calculations. Besides investigating known oxidation pathways on rhodium, such as decomposition of CH and subsequent oxidation of the decomposition products, new pathways such as direct reaction of methylidyne and oxygen toward a surface aldyhyde-type species and the decomposition of this species are considered. The unexpected and novel pathway determined here by DFT is utilized for a microkinetic model of the formation of CO and CO_2 from methylidyne. A comparison of this microkinetic study with experimental data shows that our novel mechanism can indeed describe the observations. This comparison strongly suggests that this new alternative route is the main reaction pathway for the conversion of methylidyne.

1. Introduction

Natural gas, which mainly consists of methane, often accompanies oil deposits and is furthermore a decomposition product of organic waste. Hence, it is an energy source that is available in abundance. In its raw form, however, it is frequently uneconomic to transport to the marketplace. Fortunately, natural gas can be converted into synthesis gas (syngas), a mixture of CO and hydrogen, using steam reforming or catalytic partial oxidation (CPO) over rhodium.[1−7] Synthesis gas is an attractive intermediate product for the chemical industry, since it is used for a variety of important processes such as ammonia and methanol synthesis.[8] Ammonia is a precursor for fertilizers, while methanol is a potential future fuel; the production of synthesis gas might therefore be essential for the feeding of the growing world population as well as for its energy supply. Furthermore, by oxidizing natural gas to synthesis gas and subsequent conversion into liquid fuel, via a gas-to-liquid (GTL) process such as Fischer−Tropsch synthesis,[8] the energy source can be transported much more safely via existing pipelines than is possible for gaseous natural gas. Presently, the most important industrial route to syngas is steam reforming of methane.[9] Steam reforming, however, requires large-scale converters and in addition is very energy demanding. CPO, in contrast, can be carried out in miniature reactors and is less energy demanding. The drawback of the CPO of natural gas is that it is high-temperature catalysis and syngas is rather explosive, making this process quite risky. High temperatures are compulsory for the CPO, since the reaction is thermochemically controlled. Initially, hydrocarbons are fully oxidized to CO_2 and H_2O, and the catalyst heats up rapidly owing to the strongly exothermic reactions. With increasing temperature, the system is steered in the direction of the less exothermic pathway, the formation of CO and hydrogen (the desired products). If the oxidation of CO could be kinetically blocked, however, the process could be steered to produce CO from ignition and thus could be carried out in a lower-temperature regime, making the synthesis safer. It has to be mentioned that this is a simplification of the CPO mechanism and that processes in a monolithic catalyst are much more complex: it is known for example that downstream in the catalyst, steam reforming also sets in, which affects the overall gas conversion.[10] This study, however, focuses on the surface processes inside the catalyst.

In order to steer a heterogeneously catalyzed reaction, the possible reaction pathways have to be known, enabling the scientist to determine the crucial elementary steps and to either block or enhance particular steps to steer the reaction in the desired direction. For these reasons, increasing efforts are devoted to understanding the elementary processes inside

(1) Hickman, D. A.; Haupfear, E. A.; Schmidt, L. D. *Catal. Lett.* **1993**, *17*, 223−237.
(2) Hickman, D. A.; Schmidt, L. D. *AIChE J.* **1993**, *39*, 1164−1177.
(3) Hickman, D. A.; Schmidt, L. D. Synthesis Gas-Formation By Direct Oxidation Of Methane Over Monoliths. ACS Symposium Series 523; American Chemical Society: Washington, DC, 1993, pp 416−426.
(4) Hickman, D. A.; Schmidt, L. D. *Science* **1993**, *259* (5093), 343−346.
(5) Huff, M.; Torniainen, P. M.; Hickman, D. A.; Schmidt, L. D. *Studies in Surface Science and Catalysis: Natural Gas Conversion II.* Elsevier: Amsterdam, 1994; Vol. 81, pp 315−320.
(6) Schwiedernoch, R.; Tischer, S.; Correa, C.; Deutschmann, O. *Chem. Eng. Sci.* **2003**, *58*, 633−642.
(7) Schwiedernoch, R.; Tischer, S.; Volpp, H. R.; Deutschmann, O. *Studies in Surface Science and Catalysis: Natural Gas Conversion VII*; Elsevier: Amsterdam, 2004; Vol. 147, pp 511−516.
(8) Hodnett, B. K.; Janssen, F.; Niemantsverdriet, J. W.; Ponec, V.; van Santen, R. A.; van Veen, J. A. R. Heterogeneous catalysis. In *Catalysis: An Integrated Approach*, 2nd ed.; van Santen, R. A., van Leeuwen, P. W. N. M., Moulijn, J. A., Eds.; Elsevier: Amsterdam 1999; Vol. 123, pp 209−287.
(9) van Santen, R. A.; van Leeuwen, P. W. N. M.; Moulijn, J. A. *Catalysis: An Integrated Approach*; Elsevier: Amsterdam, 2000.
(10) Horn, R.; Williams, K. A.; Degenstein, N. J.; Schmidt, L. D. *J. Catal.* **2006**, *242*, 92−102.

catalytic converters for CPO. A promising tool which could aid the development and optimization of catalytic converters are microkinetic (MK) simulations, especially when combined with computational fluid dynamics (CFD).[6,7,10,11] MK simulations, based on elementary-step surface reaction mechanisms, can predict conversions in catalytic converters accurately and, furthermore, can predict the temperature evolution of the monolith, provided that the mechanism is complete.[6] A complete mechanism is an elementary-step reaction mechanism, which includes the main surface reaction pathways and the corresponding kinetic parameters for the Arrhenius expression (activation energy as well as pre-exponential factor). Additionally, it was established recently that the activation energies of the surface reactions strongly depend on coadsorbates,[12−17] complicating the development of multistep surface reaction mechanisms. A powerful computational tool that can aid the development of those mechanisms is density functional theory (DFT), vide infra.

Numerous publications show that DFT simulations are generally very reliable in predicting preferred adsorption sites of adsorbates as well as their detailed geometries.[12,13,18,19]Owing to the constan1t acceleration of computer speed, it is now routinely possible to locate the transition state of a surface reaction on its potential energy surface (PES) and thereby to determine the corresponding activation energy.[16,20−23]

In this work the adsorption, decomposition, and oxidation of methylidyne (CH), a fragment of methane, on Rh{111} is studied. This species is generated rapidly by decomposition of CH_x ($x = 1-3$) species, which are formed upon alkane decomposition. This study focuses on the subsequent step in the reaction mechanism of hydrocarbon oxidation, because it is well-known that especially the reactions of methylidyne are the rate-determining steps.

The interaction of oxygen with Rh{111} was studied extensively experimentally (see ref 18 and references therein) as well as theoretically (see ref 12 and references therein). The nature of the interaction of methyl species with the {111} facet of rhodium is not as thoroughly studied. Mavrikakis et al. studied the adsorption and diffusion of methyl in a (2×2) symmetry cell of Rh{111}.[19] The weakening of the C−H bond upon adsorption on a Rh_{10} cluster was investigated by Chen et al.[24] Coadsorption of both species, methyl and atomic oxygen, was studied by Walter and Rappe by means of plane-wave DFT calculations.[25] Methylidyne, however, is not as well studied: Vlachos and co-workers for example calculated its binding energy on a cluster-model of a Rh{111} surface, but did not characterize the nature of the species.[26] Bunnik et al. studied the energetics of the decomposition of methane on Rh{111}.[27] In this comprehensive study the direct decomposition pathway, dehydrogenation by C−H bond breaking, is investigated; however, no alternative reaction pathways are considered. Alternative reactions of the methylidyne species are investigated in the present work and found to be of profound importance.

2. Calculation Methods

2.1. Plane-Wave Density Functional Theory. The reactions of methylidine, carbon and oxygen on Rh{111} have been studied by means of DFT calculations using Cambridge Sequential Total Energy Package (CASTEP).[28] The generalized gradient approximation (GGA) as proposed by Perdew et al. was applied,[29] combined with Vanderbilt ultrasoft pseudopotentials.[30] The plane-wave basis set was truncated at a kinetic energy of 300 eV. The reciprocal space was sampled using a *k*-point mesh with a spacing of 0.05 $Å^{-1}$ as generated by the Monkhorst−Pack scheme.[31] The surface was modeled using a four-layer rhodium slab with the lower three layers fixed at their positions in the bulk and the uppermost layer mobile. Periodic boundary conditions are used to model an extended surface. A 10-Å vacuum region was placed in between the periodic slabs to ensure that the adsorbate and the subsequent slab do not interact. Convergence tests have shown that this setup is sufficient to lead to fully converged energies, even with oxygen-containing adsorbates.

The transition state of the surface reaction was located on the potential energy surface (PES) by performing a linear synchronous (combined with quadratic synchronous) transit calculation and conjugate gradient refinements.[32]

2.2. Microkinetics. The heterogeneous kinetics are simulated using the DETCHEM software package by Deutschmann et al.,[33] based on the elementary-step reaction mechanism derived from plane-wave DFT calculations. DETCHEM uses an Arrhenius-type equation for the determination of the surface reaction rate of each elementary-step reaction, combined with a mean-field treatment of the catalytically active surface. The details of the implementation are available.[6]

3. Results and Discussion

3.1. Mechanistic Investigation. 3.1.a. Methylidyne (CH) on Rh{111}: Adsorption and Diffusion. The reactions of CH on Rh{111} are studied in the absence of hydrogen, even though hydrogen is generated during the dehydrogenation of methane. This is a justifiable assumption, because at the temperatures relevant for CPO, hydrogen will desorb rapidly.

According to our ab initio calculations, the most stable adsorption sites for the methylidyne (CH) species are the threefold hollow sites; the hcp-hollow site is more stable than

(11) Schneider, A.; Mantzaras, J.; Jansohn, P. *Chem. Eng. Sci.* **2006**, *61*, 4634−4649.
(12) Inderwildi, O. R.; Lebiedz, D.; Deutschmann, O.; Warnatz, J. *J. Chem. Phys.* **2005**, *122*, 154702.
(13) Inderwildi, O. R.; Lebiedz, D.; Deutschmann, O.; Warnatz, J. *J. Chem. Phys.* **2005**, *122*, 034710.
(14) Inderwildi, O. R.; Lebiedz, D.; Warnatz, J. *Phys. Chem. Chem. Phys.* **2005**, *7*, 2552−2553.
(15) Petersen, M. A.; Jenkins, S. J.; King, D. A. *J. Phys. Chem. B* **2006**, *110*, 11962−11970.
(16) Inderwildi, O. R.; Lebiedz, D.; Deutschmann, O.; Warnatz, J. *ChemPhysChem* **2005**, *6*, 2513−2521.
(17) Hammer, B. *Phys. Rev. B*, **2001**, *63*, 205423.
(18) Ganduglia-Pirovano, M. V.; Scheffler, M. *Phys. Rev. B: Solid State* **1999**, *59*, 15533−15543.
(19) Mavrikakis, M.; Rempel, J.; Greeley, J.; Hansen, L. B.; Norskov, J. K. *J. Chem. Phys.* **2002**, *117*, 6737−6744.
(20) Liu, Z. P.; Jenkins, S. J.; King, D. A. *J. Am. Chem. Soc.* **2004**, *126*, 10746−10756.
(21) Liu, Z. P.; Jenkins, S. J.; King, D. A. *J. Am. Chem. Soc.* **2004**, *126*, 7336−7340.
(22) Liu, Z. P.; Jenkins, S. J.; King, D. A. *J. Am. Chem. Soc.* **2003**, *125*, 14660−14661.
(23) Remediakis, I. N.; Lopez, N.; Norskov, J. K. *Angew. Chem., Int. Ed.* **2005**, *44*, 1824−1826.
(24) Chen, M.; Friend, C. M.; van Santen, R. A. *Catal. Today* **1999**, *50*, 621−627.
(25) Walter, E. J.; Rappe, A. M. *Surf. Sci.* **2004**, *549*, 265−272.
(26) Mhadeshwar, A. B.; Vlachos, D. G. *J. Phys. Chem. B* **2005**, *109*, 16819−16835.
(27) Bunnik, B. S.; Kramer, G. J. *J. Catal.* **2006**, *242*, 309−318.
(28) Segall, M. D.; Lindan, P. J. D.; Probert, M. J.; Pickard, C. J.; Hasnip, P. J.; Clark, S. J.; Payne, M. C. *J. Phys. Condens. Matter* **2002**, *14*, 2717−2744.
(29) Perdew, J. P.; Chevary, J. A.; Vosko, S. H.; Jackson, K. A.; Pederson, M. R.; Singh, D. J.; Fiolhais, C. *Phys. Rev. B: Solid State* **1992**, *46*, 6671−6687.
(30) Vanderbilt, D. *Phys. Rev. B: Solid State* **1990**, *41*, 7892−7895.
(31) Monkhorst, H. J.; Pack, J. D. *Phys. Rev. B: Solid State* **1976**, *13*, 5188−5192.
(32) Govind, N.; Petersen, M.; Fitzgerald, G.; King-Smith, D.; Andzelm, J. *Comput. Mater. Sci.* **2003**, *28*, 250−258.
(33) Deutschmann, O. http://www.detchem.com. 2001.

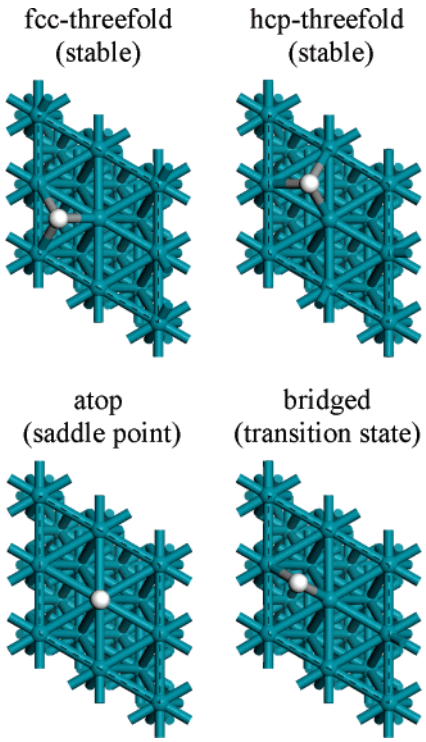

Figure 1. Top (bottom) and side (top) views of methyne in a hollow (right) and a atop (left) position on Rh{111}.

the fcc-hollow position by 0.19 eV, well in accordance with previous DFT studies.[27] In the atop position, the CH species is 2.31 eV less stable than in the hcp position and 2.12 eV less stable than in the fcc position. This immense energy difference immediately suggests that, even though this position is the result of a geometry optimization, it might not be a local energy minimum. A vibrational analysis of the atop CH species determined this species to have several imaginary frequencies, and therefore it is concluded that the atop species is actually unstable. This position can therefore act as a transition state for the diffusion of CH between threefold sites via the atop site. The activation energy for these jumps would consequently be 2.12 eV from fcc-hollow and 2.31 eV from hcp-hollow. Calculations of the PES between the atop and either hollow positions showed that it is strictly monotonic, decreasing in any direction from the atop position. This supports our conclusion that the atop position is indeed unstable and could act as a transition state for the different single-site jumps. However, as discussed below, there is an alternative preferred pathway for diffusion.

A stable, bridged CH species could not be determined on the {111} facet of rhodium. It is therefore assumed that this species acts as a transition state for the single-site jump between fcc- and hcp-hollow sites. To verify this assumption, the transition state of this single-site jump was located on the PES. This calculation confirmed that the bridged species is indeed the transition state for the diffusion of CH from one to the other hollow position and that the PES is monotonic between the bridge site and either of the hollow sites. The activation energy for this diffusion is 0.56 eV starting from the hcp-hollow position, whereas it is 0.36 eV starting from the fcc-hollow position. These barriers suggest that CH is highly mobile on Rh{111} at the temperatures considered in this study.

Table 1. Characterization of the Surface Methylidyne Species, Stable, Saddle Point and Transition State, Distances are Given in Å [10^{-9} m]

	position			
	atop	bridged	hollow	
bond length [Å]	(saddle point)	(transition state)	fcc	hcp
C−H	1.09	1.11	1.09	1.09
C−Rh	1.75	1.90	1.98	1.97
		1.91	1.99	1.98

The stable and transition-state structures are shown in Figure 1, bond lengths are given in Table 1; the calculated distances for CH in the fcc position compare very well with reported values.[27] Against this background, CH in the hcp-hollow position was chosen as the starting point for our subsequent investigations of its reactions.

3.1.b. Methylidyne Decomposition. The methylidyne decomposition was studied starting from its most stable position, the hcp-threefold site (Figure 2). Since also hydrogen is most stable in the hcp-hollow position,[34] it was assumed that, after decomposition, the hydrogen will reside in an hcp-hollow position adjacent to the formed carbon. Geometry optimization has shown that this is indeed a stable structure with a hydrogen−rhodium bond length of 1.87 Å for the rhodium atom that is not shared with the carbon atom and 1.80 Å for the bond to the shared carbon atom. The difference in the bond length can be attributed to the bonding competition.[20] The carbon−rhodium bond length decreases slightly upon C−H bond breaking; C−Rh: 1.91 Å compared to HC−Rh: 1.97/1.98 Å.

Locating the transition state of the decomposition reaction on its PES determines the activation energy of this process to be 1.28 eV (123.57 kJ/mol). The reaction is endothermic with an energy of reaction of 0.67 eV according to our calculations. The reaction parameters determined ab initio are in contrast to unity bond index-quadriatic exponential potential (UBI-QEP) estimations by Lin et al.,[35] where the activation energy was determined to be 20.93 kJ/mol (0.22 eV), clearly in marked contrast to the ab initio results. Mhadeshwar et al., however, more recently estimated the activation energy to be 115.53 kJ/mol using UBI-QEP, close to our findings.[26] Bunnik and Kramer recently determined the activation barrier to be 1.18 eV using a slightly different DFT setup.[27]

3.1.c. Hydrogen Abstraction by Coadsorbed Oxygen. A further reaction pathway toward atomic carbon is the abstraction of the hydrogen from methylidyne by an oxygen atom adsorbed in its vicinity. The products are atomic carbon and a surface hydroxyl species. Geometry optimization of this coadsorption system led to a structure in which the hydroxyl group is located in a bridged position, while carbon remains in the threefold-hcp site (Figure 3, right). The hydroxyl group is tilted with an angle of 38°. According to our first-principles calculations, this abstraction reaction has an activation energy of 1.46 eV and an energy of reaction of 0.68 eV. Again the ab initio value is far higher than the UBI-QEP value estimated by Lin et al. (0.23 eV),[35] while the estimate of 1.32 eV by Mhadeshwar et al. is in closer agreement.[26]

(34) Ciossu, L.; Inderwildi, O. R.; Lebiedz, D.; Deutschmann, O.; Warnatz, J. Spatiotemporal Monte-Carlo simulations of lateral CO/O adsorbate interactions on Rh(111) based on density functional theory computations. 2005. Manuscript submitted.
(35) Lin, Y. Z.; Sun, J.; Yi, J.; Lin, J. D.; Chen, H. B.; Liao, D. W. *J. Mol. Struct. (THEOCHEM)* **2002**, *587*, 63−71.

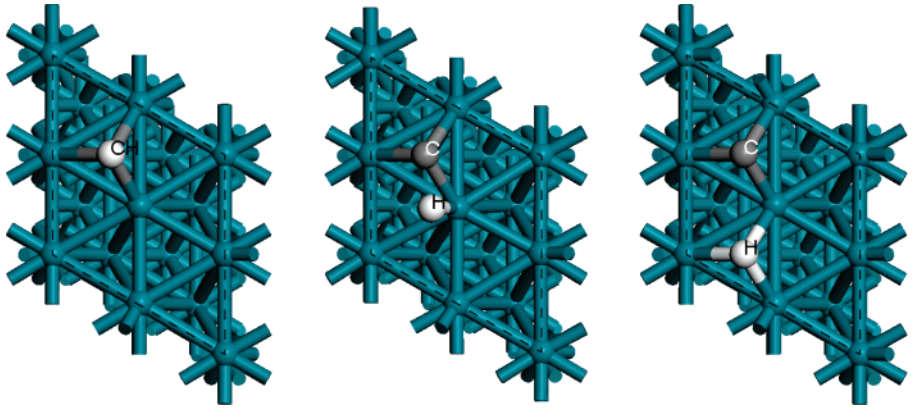

Figure 2. Decomposition of a CH species adsorbed in a threefold-hcp position; initial, transition, and final state from left to right.

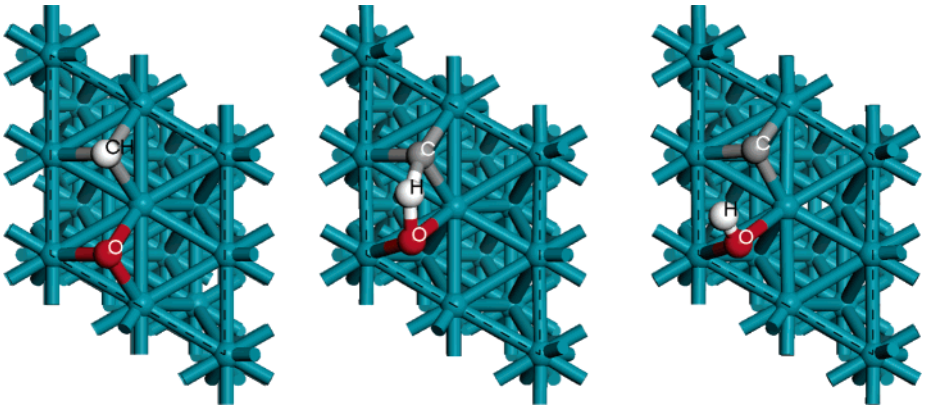

Figure 3. Abstraction of the hydrogen atom from methylidyne by a vicinal oxygen coadsorbate; initial, transition, and final state from left to right.

In the transition-state structure, the hydrogen is located between the oxygen and the carbon atom, making bond lengths of 1.33 and 1.31 Å, respectively (Figure 3, middle). Both bonds are considerably longer than regular hydrogen−oxygen and carbon−hydrogen bonds, and hence, the bonds are not covalent. This indicates that the calculated structure is indeed a genuine transition state.

Even though the activation energy of this reaction is slightly higher than the decomposition activation energy, this reaction is an alternative pathway toward surface carbon formation. Especially at high oxygen coverage, e.g., in automotive converters of lean-burn engines, this reaction will be a likely pathway in the decomposition of hydrocarbons. In both cases, the abstraction of hydrogen and the decomposition of methylidyne, the adsorbed atomic carbon so formed will be oxidized by atomic oxygen. This reaction is investigated in detail in the subsequent section.

3.1.d. Abstraction of Hydrogen by a Coadsorbed Hydroxyl Group. The hydrogen atom of a methylidyne group can also be abstracted by a coadsorbed hydroxyl group, forming water and atomic carbon. The starting point for this calculation was an atop hydroxyl group adsorbed adjacent to carbon in a threefold hollow site. In the transition-state structure, the hydrogen is located between the oxygen and the carbon atom, making bond lengths of 1.57 and 1.59 Å, respectively (Figure 4). The transition state is located rather late on the reaction coordinate (0.7), already indicating that the reaction is exothermic. The activation barrier for this reaction is 1.27 eV, and it is exothermic (−0.17 eV); the abstraction is therefore kinetically

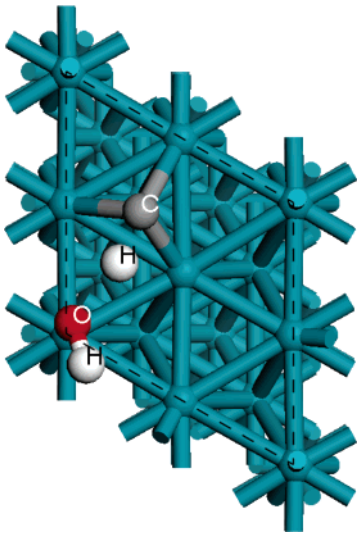

Figure 4. Transition state of the abstraction of hydrogen from CH by coadsorbed OH.

and thermochemically more likely than the decomposition of CH, according to our DFT results.

3.1.e. Carbon Monoxide Formation on Rh{111}. The formation of a surface carbonyl species (Figure 5, right) was investigated, starting from an initial state in which atomic carbon and oxygen are adsorbed in adjacent hcp positions (Figure 5, left). The transition state of the transformation leading to a CO molecule adsorbed in a hcp position was located on the PES. While carbon remains in its hollow position in the activated

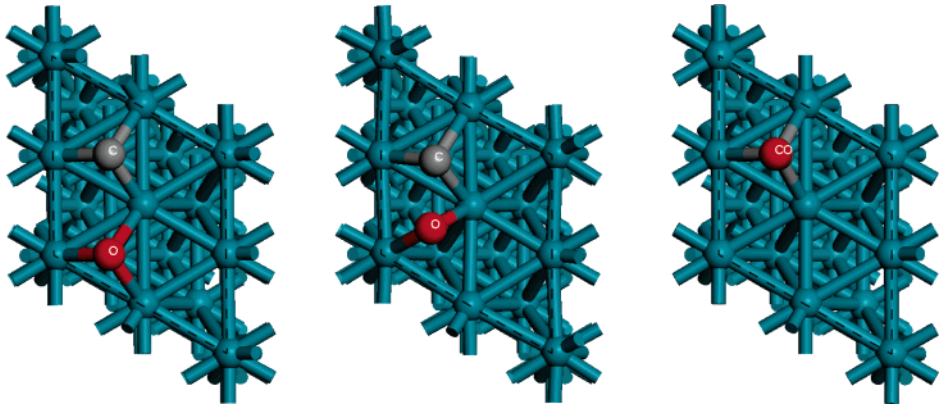

Figure 5. Oxidation of atomic carbon to carbon monoxide: initial, transition, and final state from the left to the right.

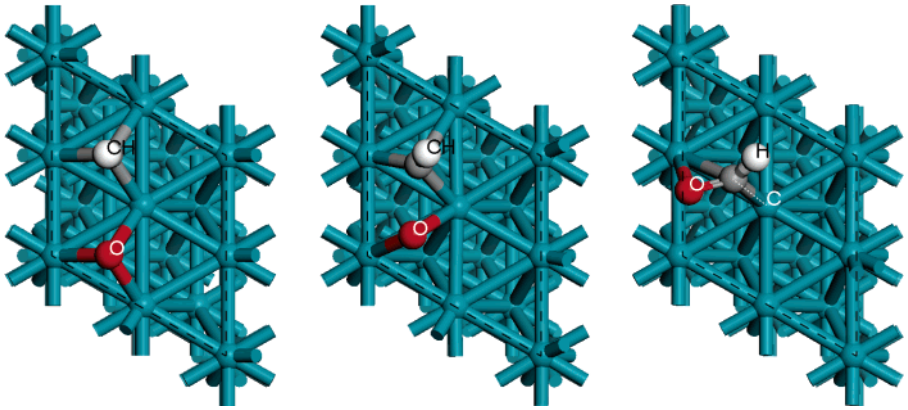

Figure 6. Reaction of oxygen with methylidyne forming a surface aldehyde species, initial, transition, and final state, from left to right.

complex, oxygen is located in a bridged position (Figure 5, middle). The calculated activation energy for this process is 0.99 eV, and the process is strongly exothermic with an energy of reaction of −2.43 eV. The exothermicity found here is in agreement with most other DFT studies,[19,36] while Liu et al. found this reaction to be endothermic using a rather similar setup.[37] Possible reasons for this discrepancy remain unclear to us, but we believe our results to be accurate. The transition state of the oxidation reaction is located at 0.25 of the reaction coordinate, in which 0 denotes the reactant geometry and 1 the product geometry. The rather low activation energy and the location of the transition state rather early on the reaction coordinate is in agreement with Hammond's postulate.[13,36,37]

The UBI-QEP investigation by Lin et al. gives an activation energy of 97.95 kJ/mol (1.01 eV) which in this case is in agreement with our ab initio study.[35] The back reaction (the carbon monoxide decomposition), however, is activated by 3.42 eV according to the DFT calculation, whereas UBI-QEP estimates the activation energy to be only 1.75 eV[35] or 2.13 eV.[26] Hence, UBI-QEP underestimates the exothermicity of the carbon oxidation drastically. Another possibility is the direct reaction of oxygen with the CH group forming an aldehyde-type surface species, considered below.

3.1.f. Direct Reaction of Methylidyne with Oxygen. An alternative reaction toward CO would be the direct reaction of CH with oxygen. According to our calculations, this reaction leads to a stable aldehyde-type surface species (Figure 6, right). This species is bonded to the surface via the carbon as well as the oxygen atom. The carbon resides in a slightly distorted bridged position with C−Rh bond lengths of 1.96 and 2.31 Å. The oxygen atom resides in a stronger distorted bridged position with O−Rh distances of 2.73 and 2.22 Å.

The aldehyde-type structure is 0.14 eV *lower* in energy than the oxygen−methylidyne coadsorption system. Since the other reactions of CH are endothermic, this pathway is the thermochemically more likely pathway, at least on this low index surface. An analogue species has already been observed experimentally on Pt{110}[38] and was confirmed theoretically by means of DFT geometry calculations.[39]

Determining the transition state on the PES for the transformation of the coadsorbates to the aldehyde-type species led to a structure in which both CH and oxygen species are located in bridged positions (Figure 6, right). The activation energy for this reaction was calculated to be 1.15 eV, making it also kinetically the most probable pathway. The transition state is located rather early on the reaction coordinate, and therefore, the rather low activation energy as well as the exothermicity are in agreement with Hammond's postulate.[36,37]

The exothermictiy and the relatively low activation barrier (which is lower than the activation barrier of the "classic" pathway) suggests that this reaction should be considered in microkinetic simulations of hydrocarbon oxidation reaction over rhodium. In order to proceed with this assumption, the competitive process leading to the decomposition of the aldehyde species was investigated.

(36) Hammer B. *Top. Catal.* **2006**, *37*, 3−16.
(37) Hammond, G. S. *J. Am. Chem. Soc.* **1955**, *77*, 334−338.
(38) Watson, D. T. P.; Harris, J. J. W.; King, D. A. *Surf. Sci.* **2002**, *505*, 58−70.
(39) Petersen, M. A.; Jenkins, S. J.; King, D. A. Manuscript in preparation.

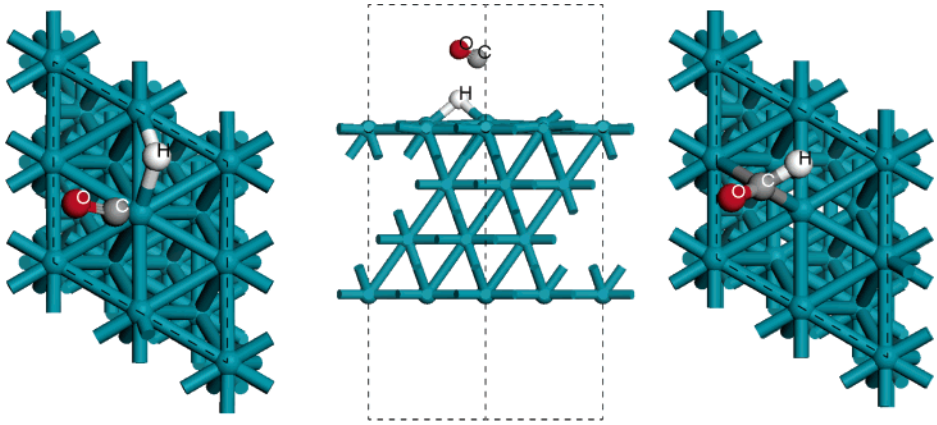

Figure 7. Transition state of the decomposition of surface CHO to adsorbed CO and H (right) and to adsorbed H and gas-phase CO (left: top view, middle: side view).

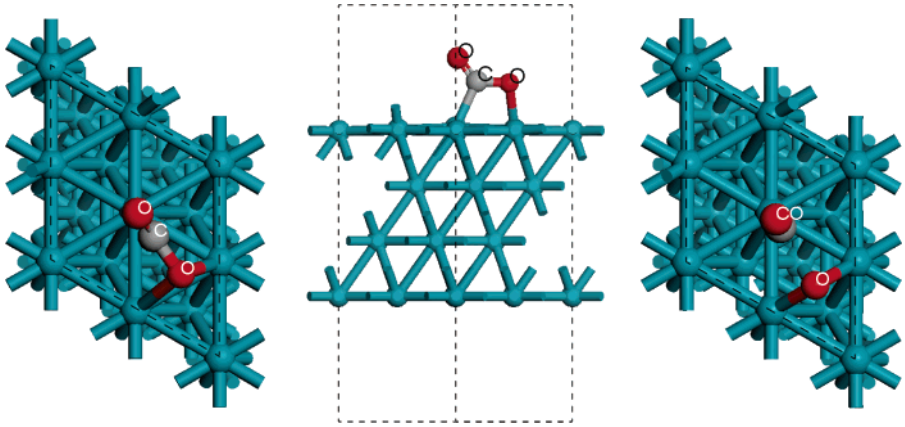

Figure 8. Surface carboxylic anhydride species (left: top view, middle: side view) and the transition state of its formation from coadsorbed CO and O (right).

3.1.g. Decomposition of the Surface Aldehyde Species. Two scenarios have to be considered: the aldehyde species can decompose on the surface, leading to coadsorbed hydrogen and CO, and it can decompose to form gas-phase CO thus leaving hydrogen behind on the surface. In order to verify which pathway is the most likely, the transition states of both were determined (Figure 7). In case of the decomposition forming exclusively adsorbed species, the activation barrier is 0.3 eV and the reaction is *markedly* endothermic with a reaction energy of −1.33 eV. The subsequent desorption of CO is activated by 2.07 eV, whereas the oxidation is activated by 0.99 eV. The oxidation is therefore kinetically favored, leading to a preferential formation of CO_2 in the kinetically controlled regime; if this could be reversed, catalysts could be tuned to yield CO preferentially. Recent results indicate that bimetallic systems could be the key to this problem, because they *drastically* alter the adsorption properties of diatomic molecules; this study therefore goes hand-in-hand with ongoing research on bimetallic surfaces.[40]

The direct formation of gas-phase CO from CHO has an activation barrier of 0.84 eV, and the reaction is endothermic (0.72 eV). In the transition state the hydrogen is located in a bridged position, and the hydrogen−carbon distance lengthens significantly to 2.48 Å in the transition state compared to 1.10 Å in the precursor. The H−Rh distances in the transition state are 1.85 and 1.69 Å, and the final state H resides in a hollow position with a H−Rh distance of 1.85 Å.

Even though the formation of CO via pathway B is overall kinetically favored, the first step of pathway A is kinetically and thermochemically more probable, and therefore the reaction will proceed in this direction in the low-temperature regime. It is furthermore sensible to assume that during the high-temperature oxidation of methane on Rh{111} both pathways have to be considered. The difference between these two processes is that, in pathway A, CO remains on the surface, whereas in pathway B, gas-phase CO is formed. Since CO on the surface can easily be oxidized to CO_2, vide infra, pathway B might provide an opportunity to steer the oxidation of hydrocarbons in the direction of the desired CO.

3.1.h. Further Reactions of the Aldehyde Species. The aldehyde species can obviously also react with further coadsorbates such as oxygen. This reaction would, according to our calculations, lead to a surface formic carboxylate species (i.e., formate). The reaction has, however, a rather high activation barrier of 1.42 eV, compared to 0.3 eV for the on-surface dissociation of CHO. This, combined with the fact that CPO is a high-temperature, low-coverage process (and hence two subsequent collisions with oxygen are not very likely), leads to the conclusion that such a species can be excluded as an intermediate in a main reaction path. It can, however, explain why minor amounts of formic acid are observed in CPO

(40) Inderwildi, O. R.; Jenkins, S. J.; King, D. A. 2006. Manuscript submitted.

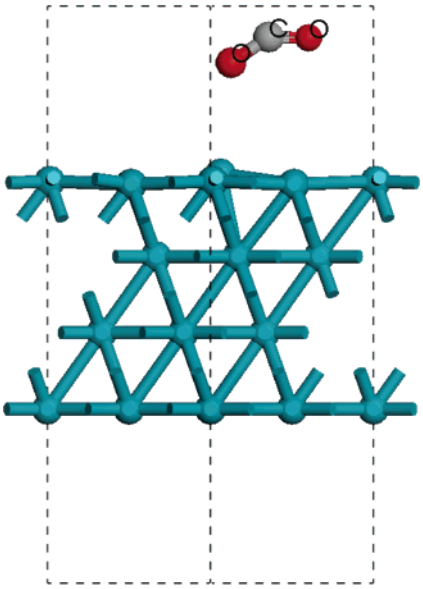

Figure 9. Transition state of the formation of gas-phase CO_2 from a surface carboxyl anhydride species.

Table 2. Improved Reaction Mechanism for the Oxidation of Methylidyne, Origin of the Parameters Is Given on the Right-Hand Side

process	A [mol, cm, s]	E_a [kJ mol^{-1}]	ref
Desorption			
$CO_{(s)} \rightarrow Rh_{(s)} + CO$	3.5×10^{13}	133.4	43
$CO^*_{(s)} \rightarrow Rh_{(s)} + CO^*$	3.5×10^{13}	133.4	43
$CO_{2(s)} \rightarrow Rh_{(s)} + CO_2$	1.0×10^{13}	21.7	*a*
$CHO_{(s)} \rightarrow CO^* + H_{(s)}$	1.0×10^{13}	80.9	*a*
$H_2O_{(s)} \rightarrow Rh_{(s)} + H_2O$	3.0×10^{13}	45.0	6
$H_{(s)} + H_{(s)} \rightarrow H_2 + Rh_{(s)} + Rh_{(s)}$	3.0×10^{21}	77.8	6
$O_{(s)} + O_{(s)} \rightarrow O_2 + Rh_{(s)} + Rh_{(s)}$	1.3×10^{22}	355.2	6
Surface Reactions			
$CH_{(s)} + Rh_{(s)} \rightarrow C_{(s)} + H_{(s)}$	3.7×10^{21}	123.0	*a*
$C_{(s)} + H_{(s)} \rightarrow CH_{(s)} + Rh_{(s)}$	3.7×10^{21}	58.0	*a*
$CH_{(s)} + O_{(s)} \rightarrow CHO_{(s)} + Rh_{(s)}$	3.7×10^{21}	111.0	*a*
$CHO_{s)} + Rh_{(s)} \rightarrow CO^*_{(s)} + H_{(s)}$	3.7×10^{21}	28.9	*a*
$CH_{(s)} + O_{(s)} \rightarrow C_{(s)} + OH_{(s)}$	3.7×10^{21}	141.0	*a*
$CH_{(s)} + OH_{(s)} \rightarrow C_{(s)} + H_2O_{(s)}$	3.7×10^{21}	122.0	*a*
$C_{(s)} + O_{(s)} \rightarrow CO_{(s)} + Rh_{(s)}$	3.7×10^{21}	95.4	*a*
$CO_{(s)} + O_{(s)} \rightarrow CO_{2(s)} + Rh_{(s)}$	3.7×10^{21}	128.0	*a*
$CO^*_{(s)} + O_{(s)} \rightarrow CO_{2(s)} + Rh_{(s)}$	3.7×10^{21}	128.0	*a*
$CO_{2(s)} + Rh_{(s)} \rightarrow CO_{(s)} + O_{(s)}$	3.0×10^{21}	57.0	6/*a*
$CO_{(s)} + Rh_{(s)} \rightarrow C_{(s)} + O_{(s)}$	3.0×10^{22}	329.0	6/*a*
$CO^*_{(s)} + Rh_{(s)} \rightarrow C_{(s)} + O_{(s)}$	3.0×10^{22}	329.0	6/*a*
$H_{(s)} + O_{(s)} \rightarrow OH_{(s)} + Rh_{(s)}$	5.0×10^{22}	83.7	6
$OH_{(s)} + Rh_{(s)} \rightarrow H_{(s)} + O_{(s)}$	3.0×10^{20}	37.7	6
$H_{(s)} + OH_{(s)} \rightarrow H_2O_{(s)} + Rh_{(s)}$	3.0×10^{20}	33.5	6
$H_2O_{(s)} + Rh_{(s)} \rightarrow H_{(s)} + OH_{(s)}$	5.0×10^{22}	106.4	6
$OH_{(s)} + OH_{(s)} \rightarrow H_2O_{(s)} + O_{(s)}$	3.0×10^{21}	100.8	6
$H_2O_{(s)} + O_{(s)} \rightarrow OH_{(s)} + OH_{(s)}$	3.0×10^{21}	224.2	6

[a] Refers to values derived from this work: activation barriers from DFT and pre-exponential factors from transition state theory.

experiments and why catalysts can be tuned to produce formate preferentially.[41,42] A detailed study of this side process is, however, outside the scope of this work.

3.1.i. Formation and Desorption of Carbon Dioxide. According to our calculations, CO is most easily oxidized when it is absorbed in an atop fashion. Oxygen attacks the partially positively charged carbon atom, and a surface carboxylic anhydride species is formed (Figure 8). The carboxylic anhydride species resides in a hollow position with the oxygen located in a bridged position (Rh−O: 2.17 Å) and the carboxyl group located in an atop position (Rh−C: 2.00 Å), forming a bridge over the hollow site (C−O: 1.30 Å). Locating the transition state of the oxidation on the PES leads to an activated complex in which the attacking O is in a bridged site and CO in an atop, leaning toward the O (Rh−C: 1.91 Å; Rh−O: 2.00 Å; C−O 1.16 Å).

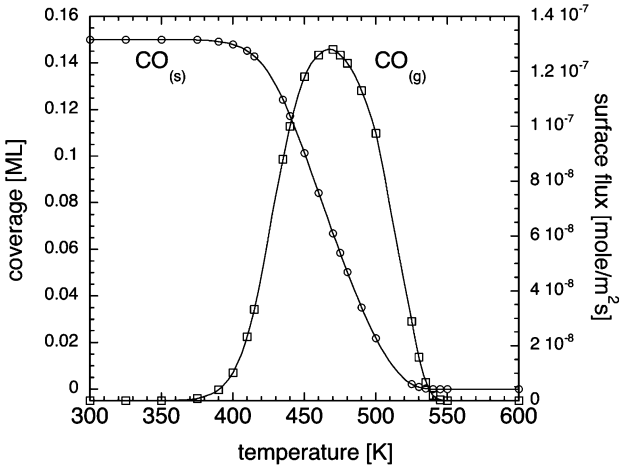

Figure 10. Simulated TPD spectra of 0.15 ML CO on Rh{111}.

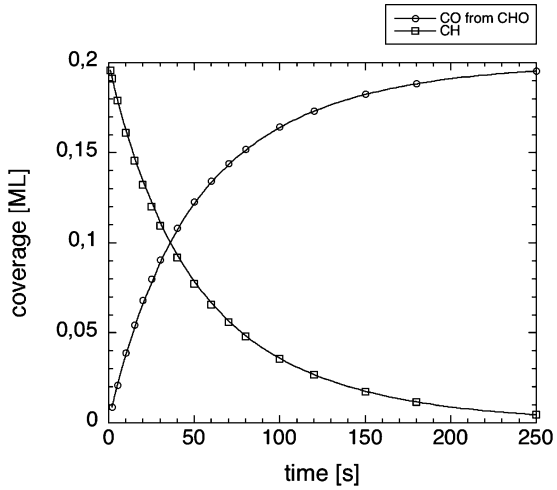

Figure 11. CH consumption and CO formation on Rh{111} at 400 K as function of time using the mechanism developed in this work by means of DFT.

The reaction has an activation barrier of 1.13 eV (108.50 kJ mol^{-1}) (significantly higher than the E_A of the decomposition of CHO) and is endothermic (0.55 eV). The transition state is depicted in Figure 8 on the right. The back reaction is consequently exothermic and has an activation barrier of 0.58 eV.

The desorption of the surface CO_2 species formed in this reaction is exothermic (−0.13 eV), and the desorption process has, according to our DFT calculations, a real transition state and a rather high activation barrier of 1.17 eV. This is not too surprising, since this desorption process not only cleaves an adsorbate−surface bond, but also includes π-bond formation and consequently rehybridization. In the activated complex the CO_2 is, as expected, not linear but bent (144°), and one of the CO bonds is 1.35 Å longer than a C−O double bond, indicating

(41) Larkin, D. W.; Lobban, L. L.; Mallinson, R. G. *Catal. Today* **2001**, *71*, 199−210.
(42) Parmaliana, A.; Frusteri, F.; Arena, F.; Mezzapica, A.; Sokolovskii, V. *Catal. Today* **1998**, *46*, 117−125.

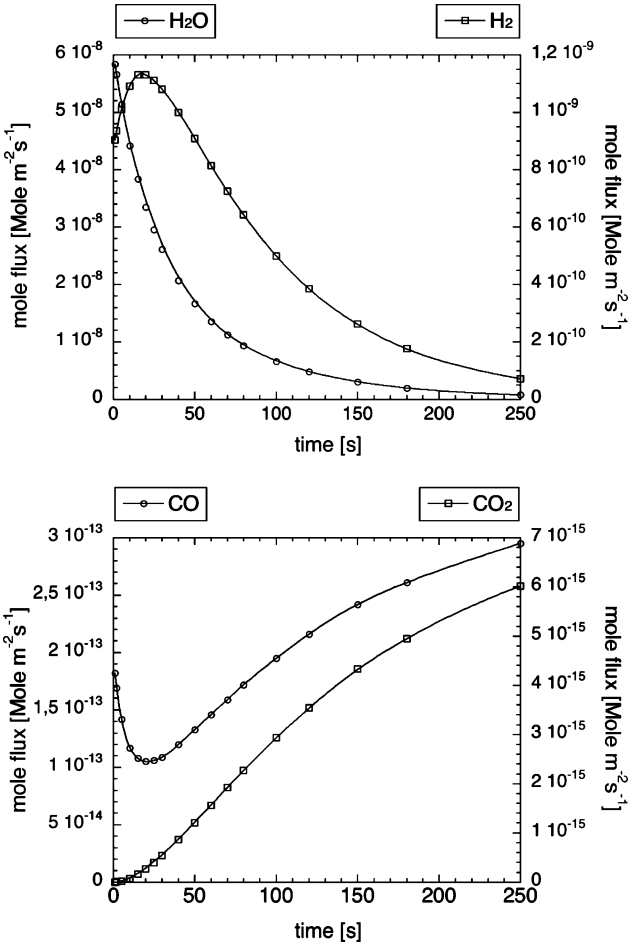

Figure 12. Surface mole flux of water and hydrogen (top) and CO and CO_2 (bottom) as a function of time over a surface precovered with 0.7 ML oxygen and 0.2 ML methylidyne.

a genuine transition state. The decomposition of the CO_2 species is kinetically and thermochemically favored. If it would be possible to either hinder oxidation or enhance the decompositon of the surface carboxylic anhydride species, the reaction could be steered into the direction of CO formation (Figure 9). This in addition to a possible enforcement of the direct decomposition of the surface aldehyde species, vide supra, could enforce the preferential formation of CO and thereby lower the temperature of the partial oxidation of hydrocarbons.

3.2. Kinetic Modeling. The presented DFT results strongly suggest that on Rh{111} the main reaction pathway of CO formation is via the aldehyde species as opposed to the decomposition of CH and subsequent oxidation of atomic carbon by oxygen.

In order to support this assumption, microkinetic simulations of the temperature programmed desorption (TPD) of CO and the temperature programmed reaction (TPR) of methylidyne and oxygen were carried out. Since it is well-known that DFT calculations overestimate the adsorption energies of molecules on metal surfaces, the desorption energy of CO from Rh{111} and its coverage dependence were taken from ref 43. The

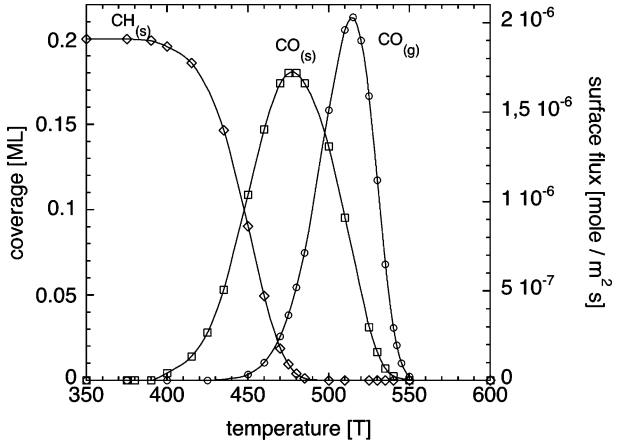

Figure 13. Surface coverage of CH and CO as well as surface flux of CO as a function of the surface temperature.

complete mechanism and the corresponding kinetic parameters are given in Table 2.

The simulated TPD spectra of 0.15 ML CO on Rh{111} is shown in Figure 10; the desorption sets in at ~400 K, in agreement with Schennach et al.,[43] the desorption peaks at 480 K, slightly below the desorption temperature of 490 K determined by Somorjai and co-workers, while slightly above the 470 K reported by Thiel et al.[44]

Subsequently, the surface reaction of a surface covered with 0.2 ML CH and 0.7 ML oxygen was simulated. CO generated from an aldehyde species is labeled in the subsequent reactions to determine through which pathway the CO was formed. The simulation was carried out at 400 K, because this temperature is sufficient to decompose CH and to form the aldehyde species, but below the light-off temperature of the CO oxidation and the initiation of CO desorption. As can be seen from Figure 11, the surface CO is exclusively formed via the aldehyde pathway, and formation of surface carbon is negligible, first, because the activation barrier is higher than the barrier to aldehyde formation and, second, the reaction is endothermic and consequently the back-reaction has a much lower activation energy. Since the barrier to decomposition of CHO via both pathways is much lower than the barrier of the formation of the species itself and 0.14 eV are generated upon CHO formation, the concentration of the surface aldehyde is negligible.

A simulation of the mole flux of the different species generated shows that these simulations can very well describe a shift from H_2 to H_2O production as well as a shift from CO_2 to CO, exactly as observed by experiment.[6] In Figure 12 the mole flux over the surface is given as function of time; from the upper graph it can be seen that initially water is formed, but the water flux at the surface decreases exponentially, while the hydrogen flux increases due to the shift of the reaction from kinetic to thermochemical control. Hydrogen formation peaks at ~30 s and decreases afterward, owing to the consumption of the surface methylidyne species. The same shift of the reaction pathway can be seen for CO and CO_2: initially CO is formed, and the slightly exothermic reaction provides the energy for the ignition of CO oxidation, which becomes manifest in the formation of CO_2. After the ignition of CO_2 formation both species are formed and desorb simultaneously, but the equilib-

(43) Schennach, R.; Krenn, G.; Klotzer, B.; Rendulic, K. D. *Surf. Sci.* **2003**, *540*, 237−245.
(44) Thiel, P. A.; Williams, E. D.; Yates, J. T., Jr.; Weinberg, W. H. *Surf. Sci.* **1979**, *84*, 54−64.

rium favors CO formation, in accordance with experimental studies of the ignition process.

In order to verify the calculated kinetic parameters with experimental data, a temperature-programmed reaction−desorption spectrum of the studied system was simulated. It can be seen from Figure 13 that initially CH is consumed (light-off at 440 K) and adsorbed CO forms. The CO generated is almost exclusively via the novel aldehyde pathway. At 400 K desorption of CO sets in and peaks at approximately 515 K. The center of the simulated desorption peak is at 495 K, which is in very good agreement with the experimentally determined value of 490 K.[45] This excellent agreement with experimental data further supports our newly developed mechanism. To firmly establish this reaction route, however, further experimental work is necessary.

4. Summary and Conclusion

The present study investigates the oxidation of CH on Rh{111}. These steps are of utmost importance for the microkinetic modeling of hydrocarbon oxidation since they are part of the product selection and rate-determining steps, apart from methane dissociative adsorption. Calculated activation energies for the elementary steps partially support mechanisms used in the literature, which are based on approximations made with UBI-QEP. The activation energy of the oxidation of atomic carbon for example is supported by plane-wave DFT calculations. However, other activation energies for elementary reactions such as hydrogen abstraction and CH decomposition determined via UBI-QEP do not agree even approximately with our first-principles results.

Apart from the common elementary reactions, a novel pathway, not previously considered in microkinetic models, is found. This pathway, involving the formation of an aldehyde-type surface species, is kinetically as well as thermodynamically more likely than the usual reaction step, according to our DFT results. Microkinetic simulations based on this mechanism, as improved by our DFT investigation, support our assumption that decomposition of CH and subsequent oxidation of the decomposition products is not the main reaction pathway of hydrocarbon oxidation. CO and CO_2 formed are, according to our microkinetic study, almost exclusively generated via the surface aldehyde species. By contrast the amount formed via CH decomposition is negligible. We emphasize that we are aware of the fact that the TPD spectrum can also be simulated using the "conventional" mechanism; nevertheless, our mechanism is based on first-principles results, whereas the kinetic parameters of the conventional mechanism are fitted or estimated.

This study gives therefore further insight into the hydrocarbon oxidation on Rh{111} and will therefore aid the development of elementary-step reaction mechanisms, not only for CPO but also for other processes such as automotive emission control. Furthermore, the crucial steps of the partial and full oxidation processes provide a basis for analyzing a possible blocking/enhancement to steer the reaction in the direction of the desired partial oxidation product. If a bimetallic system could be found that stabilizes methylidyne and enhances direct CO formation from CHO, the catalytic partial oxidation could be carried out under milder conditions, which are less costly and, more importantly, less dangerous.

The influence of surface defects such as steps and kinks is also of crucial importance for a comprehension of heterogeneous catalysis.[16,22] A thorough study of hydrocarbon decomposition and oxidation on stepped rhodium surfaces is therefore currently in progress.

Acknowledgment. We acknowledge the German Research Foundation (DFG) for a postdoctoral fellowship (O.R.I.), The Royal Society for a University Research Fellowship (S.J.J.), and Heidelberg Linux Cluster (HELCIS) for computation time.

JA067722W

(45) Crowell, J. E.; Somorjai, G. A. *J. Vac. Sci. Technol., A* **1984**, *2*, 881−882.